Heat Mass Transfer (2006) 42: 311–321
DOI 10.1007/s00231-005-0014-5

ORIGINAL

Abdullatif Ben-Nakhi · Ali J. Chamkha

Natural convection in inclined partitioned enclosures

Received: 18 October 2004 / Accepted: 5 July 2005 / Published online: 10 November 2005

Abstract The problem of steady, laminar, natural convective flow of a viscous fluid in an inclined enclosure with partitions is considered. Transverse gradient of temperature is applied on the two opposing regular walls of the inclined enclosure while the other walls are maintained adiabatic. The problem is formulated in terms of the vorticity-stream function procedure. A numerical solution based on the finite volume method is obtained. Representative results illustrating the effects of the enclosure inclination angle and the degree of irregularity on the contour maps of the streamlines and temperature are reported and discussed. In addition, results for the average Nusselt number at the heated wall of the enclosure and the difference of extreme stream-function values are presented and discussed for various Rayleigh numbers, inclination angles and dimensionless partition heights.

Nomenclature

A	Enclosure system's aspect ratio = L/H
B	Dimensionless partition height, h/H
g	Gravitational acceleration
h	Partition height
H	Enclosure system's height
l	Partition length
L	Enclosure system's total length
n	Normal direction
$\overline{\mathrm{Nu}}$	Average Nusselt number at heated wall
p	Fluid pressure
Pr	Prandtl number = ν/α_t
Ra	Thermal Rayleigh number = $g\beta_T(T_h - T_c)H^3/(\alpha_t \nu)$
t	Time
T	Temperature
T_h	Hot wall temperature (source)
T_c	Cold wall temperature (sink)
u	x-component of velocity
U	Dimensionless X-component of velocity = uH/α_t
v	y-component of velocity
V	Dimensionless Y-component of velocity = vH/α_t
x	Distance along insulated walls
X	Dimensionless distance along insulated walls = x/H
y	Distance normal to insulated walls
Y	Dimensionless distance normal to insulated walls = y/H

Greek Symbols

α	Enclosure inclination angle
α_t	Thermal diffusivity
β_T	Thermal expansion coefficient
ν	Kinematic viscosity
θ	Dimensionless temperature = $(T - T_c)/(T_h - T_c)$
ρ	Density
τ	Dimensionless time = $\alpha_t t/H^2$
Ω	Vorticity
ψ	Dimensionless stream function = Ψ/α_t
Ψ	Stream function
ζ	Dimensionless vorticity = $\Omega H^2/\alpha_t$
∇^2	Laplacian operator

A. Ben-Nakhi
Mechanical Power & Refrigeration Department,
The Public Authority for Applied Education and Training,
P. O. Box 42325, Shuweikh, 70654 Kuwait

A. J. Chamkha (✉)
Manufacturing Engineering Department,
The Public Authority for Applied Education and Training,
P. O. Box 42325, Shuweikh, 70654 Kuwait
E-mail: chamkha@paaet.edu.kw

1 Introduction

Buoyancy-induced flow and heat transfer in different finite geometries has been the subject of many research investigations. This interest stems from the significance of buoyancy-induced flows in various engineering and technological applications such as convective heat loss

from solar collectors, thermal insulation, nuclear reactors, heat-recovery systems, energy conservation in buildings, air conditioning and ventilation, cooling of electronic equipments, crystal growth and semiconductor production. The books by Bejan [1], Platten and Legros [2] and Yang [3] report reviews on various investigations dealing with natural convection heat transfer.

For many years, natural convection from differentially heated rectangular cavities over a range of Rayleigh numbers has received considerable attention. De Vahl Davis and Jones [4] Jones [5], Saitoh and Hirose [6], and De Vahl Davis [7] have considered various aspects and comparisons of steady-state natural convection of air in a square cavity. Chenoweth and Paolucci [8] and Paolucci and Chenoweth [9] have studied transient natural convection in an enclosed vertical air layer with large horizontal temperature differences. Le Quere and Roquefort [10] have solved unsteady natural convection in two-dimensional cavities with Chebyshev polynomials. This problem was also solved for different Prandtl number by Gresho et al. [11], Marshall et al. [12] and Usmani [13]. Catton [14] has studied the effect of wall conduction on the stability of a fluid in a rectangular region heated from below and has reported a review on natural convection in enclosures [15]. Oertel [16] has considered steady and time-dependent convection in a rectangular box. Torrance [17] has reported on natural convection in thermally stratified enclosures with localized heating from below. Kamotani et al. [18] have studied natural convection heat transfer in a water layer with localized heating from below. Also, Fusegi and Farouk [19] have analyzed natural convection in a thermally stratified square cavity with localized heating from below.

Furthermore, various studies dealing with natural convection in inclined enclosures have been reported. These studies show that tilting the enclosure have significant effect on the flow and heat transfer characteristics. For instance, in crystal growth processes from melts, it has been reported by Markham and Rosenberger [20] that larger transport rated are obtained by tilting the ampoule. Motivated by this, Bontoux et al. [21] have carried out a numerical and experimental investigation on three-dimensional buoyancy-driven flows in a tilted cylinder (ampoule) with axial heating. Many other examples on the effect of inclination on natural convection flows have been reported by Delgado-Buscalioni and Crespo del Arco [22]. For example, it has been proven that significant heat transfer enhancement can be obtained when the tube in a heat exchanger is optimally inclined (see Lock and Fu [23]). Wirtz and Tsheng [24, 25] have studied natural convection across tilted rectangular enclosures of small aspect ratio. Also, Cerisier and Rahal [26] have employed inclined geometries in their experimental investigation on natural convection in enclosures with axial and lateral heating to study the interaction between longitudinal and transversal instabilities.

Owing to various applications, interest in the study of natural convection heat transfer in repetitive or irregularly partitioned geometries has increased in recent years. For example, the easiest way to remove the heat generated by the presence of many elements in an electronic circuit board is accomplished by natural convection. The rate of heat transfer through an enclosure may be controlled by the presence of dividers within the enclosure. The length, thickness and location of the dividers can have a significant effect on the heat transfer and fluid flow in the enclosure. Jacobs et al. [27] have considered the case of a fluid mass of infinite extent above an array of uniformly spaced rectangular cavities. The bottom of the cavities was assumed to be isothermal with either adiabatic or isothermal sidewalls. Later, the same problem was reconsidered by Jacobs and Mason [28] with the bottom of the cavities subjected to a uniform heat flux rather than constant temperature. They have found that the imposition of a uniform heat flux at the bottom of the cavities lead to the development of strong secondary flow circulation cells and, ultimately, to a reversal flow in the cavity. Hasnaoui et al. [29] have later considered natural convection above an array of open cavities heated from below. They have found that the transition to steady-state flow sustained oscillatory behavior in several cases. Jetli et al. [30] have studied the influence of baffle location on natural convection in a partially divided enclosure. Raji et al. [31] have analyzed natural convection in interacting cavities heated from below. They have found that the symmetry of the solutions is considerably affected by the relative height of the cavities and their number. Dagtekin and Oztop [32] have investigated natural convection heat transfer by heated partitions within an enclosure. They have found that as the partitions, height increases, the mean Nusselt number increases and that the position of partitions have more effects on fluid flow than that of heat transfer. More recently, Yucel and Ozdem [33] have studied natural convection in partially divided square enclosures. They have concluded that the mean Nusselt number decreases with increasing the height and number of partitions.

Motivated by the above investigations, the objective of this work is to consider laminar, two-dimensional natural convection flow due to sidewalls temperature gradient inside an inclined partitioned enclosure. The upper and bottom walls are assumed to be insulated. Three repetitive insulated partitions (cavities) exist along the bottom wall of the major enclosure. Various aspect ratios of these partitions will be considered in the present work.

2 Mathematical model

Consider steady laminar, two-dimensional, natural convective flow inside an inclined partitioned enclosure. The temperatures T_h and T_c are uniformly imposed on two opposing walls such that $T_h > T_c$ while the other

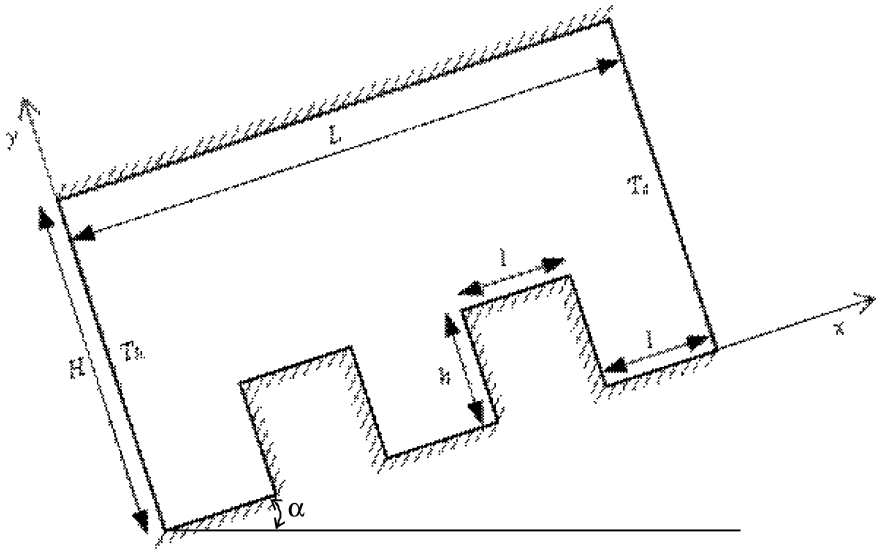

Fig. 1 Problem schematic and coordinate system

walls are assumed to be adiabatic. Figure 1 shows the schematic and coordinate system of the problem under consideration. The fluid is assumed to be incompressible, Newtonian and viscous has constant thermo-physical properties except the density in the buoyancy term of the momentum equations. The effect due to viscous dissipation is assumed to be negligible.

The governing equations for this problem are based on the balance laws of mass, linear momentum and energy. Taking into account the assumptions mentioned above, and applying the Boussinesq approximation for the body force terms in the momentum equations, the governing equations can be written in dimensionless stream function–vorticity form as:

$$\zeta = \frac{\partial V}{\partial X} - \frac{\partial U}{\partial Y} = -\nabla^2 \psi, \tag{1}$$

$$\frac{\partial \zeta}{\partial \tau} + U\frac{\partial \zeta}{\partial \mathrm{X}} + V\frac{\partial \zeta}{\partial \mathrm{Y}} = \mathrm{Pr}\,\nabla^2\zeta + \mathrm{Ra}\,\mathrm{Pr}\cos\alpha\left(\frac{\partial \theta}{\partial \mathrm{X}}\right) - \mathrm{Ra}\,\mathrm{Pr}\sin\alpha\left(\frac{\partial \theta}{\partial \mathrm{Y}}\right), \tag{2}$$

$$\frac{\partial \theta}{\partial \tau} + U\frac{\partial \theta}{\partial X} + V\frac{\partial \theta}{\partial Y} = \nabla^2\theta, \tag{3}$$

where the dimensionless stream function and vorticity are defined in the usual way as

$$U = \frac{\partial \psi}{\partial \mathrm{Y}}, \quad V = -\frac{\partial \psi}{\partial \mathrm{X}}, \quad \zeta = -\left(\frac{\partial^2 \psi}{\partial \mathrm{X}^2} + \frac{\partial^2 \psi}{\partial \mathrm{Y}^2}\right). \tag{4}$$

In writing Equations (1) through (4), the following dimensionless parameters are employed:

$$X = \frac{x}{H}, \quad Y = \frac{y}{H}, \quad \tau = \frac{\alpha_t t}{H^2}, \quad \zeta = \frac{\Omega H^2}{\alpha_t}, \quad \psi = \frac{\Psi}{\alpha_t}, \quad \theta = \frac{(T - T_c)}{(T_h - T_c)}, \quad \mathrm{Pr} = \nu/\alpha_t, \quad \mathrm{Ra} = \frac{g\beta_T (T_h - T_c) H^3}{\alpha_t \nu}, \tag{5}$$

where all parameters appearing in the above equations are given in the Nomenclature list.

The appropriate initial and boundary conditions for the problem under consideration can be written in dimensionless form as:

$$U = V = \psi = \theta = 0 \quad \text{for } \tau = 0 \tag{6a}$$

$X = 0$:

$$U = V = \psi = 0, \quad \zeta = -\left(\frac{\partial^2 \psi}{\partial X^2}\right), \quad \theta = 1 \tag{6b}$$

$X = A$:

$$U = V = \psi = 0, \quad \zeta = -\left(\frac{\partial^2 \psi}{\partial X^2}\right), \quad \theta = 0. \tag{6c}$$

Insulated walls:

$$U = V = \psi = 0, \quad \zeta = -\left(\frac{\partial^2 \psi}{\partial Y^2}\right), \quad \frac{\partial \theta}{\partial \mathrm{n}} = 0, \tag{6d}$$

where $A = L/H$ is the enclosure system's aspect ratio and n is the normal direction.

Equations (2) and (3) governing ζ and θ can be cast in the general canonical form (see Patankar [34]) as:

$$\frac{\partial \phi}{\partial \tau} + \frac{\partial}{\partial X}\left[\mathrm{U}\phi - \Gamma_\phi \frac{\partial \phi}{\partial X}\right] + \frac{\partial}{\partial Y}\left[V\phi - \Gamma_\phi \frac{\partial \phi}{\partial Y}\right] = S_\phi, \tag{7}$$

where ϕ stands for ζ or θ and Γ ϕ and S_ϕ are given by

$$\Gamma_\theta = 1, \; S_\theta = 0,$$

$$\Gamma_\zeta = \mathrm{Pr}, \quad \mathrm{S}_\zeta = \mathrm{Pr}\,\mathrm{Ra}\left[\frac{\partial \theta}{\partial \mathrm{X}}\cos\alpha - \frac{\partial \theta}{\partial Y}\sin\alpha\right]. \tag{8}$$

The average Nusselt number at the heated wall of the enclosure system is given by:

$$\overline{\mathrm{Nu}} = -\int_0^1 \left(\frac{\partial\theta}{\partial \mathrm{X}}\right) \mathrm{d}Y \tag{9}$$

3 Numerical algorithm

In the present work, the boundary-value problem represented by (1) through (3) is solved subject to its corresponding initial and boundary conditions given in (6) by the control-volume method discussed by Patankar [34]. In this method, the ADI procedure along with the Successive Over-Relaxation (SOR) scheme is implemented in the spatial and temporal environments, respectively, to accelerate the convergence of the solution towards steady state. Additionally, the application of the ADI procedure enhances the accuracy of the solution since it allows the power-law scheme to be applied locally in a one-dimensional sense for each sweep in the coordinate directions. In order to test and assess grid independence of the solution scheme, many numerical experiments were performed. These experiments showed that, in general, an equally spaced grid mesh of 121×65 is adequate to describe the flow and heat-transfer characteristics accurately. Further increase in the number of grid points produced essentially the same results. The convergence criterion employed to reach the steady-state solution was the standard relative error, which is based on the maximum norm given by

$$\Delta = \frac{\left\|\zeta^{m+1} - \zeta^{m}\right\|_\infty}{\left\|\zeta^{m+1}\right\|_\infty} + \frac{\left\|\theta^{m+1} - \theta^{m}\right\|_\infty}{\left\|\theta^{m+1}\right\|_\infty} \leq 10^{-6}, \tag{10}$$

where the operator $\|\eta\|_\infty$ indicates the maximum absolute value of the variable over all the grid points in the computational domain and m and $m+1$ represent the old time and advanced time step, respectively.

The accuracy of numerical scheme is validated by comparing the present results with various cases of the problem of Raji et al. [31] who considered a configuration that is very similar to the present geometry, and excellent agreement is observed as is evident from Figs. 2a-c. These favorable comparisons lend confidence in the numerical results to be presented in the next section.

4 Result and discussion

In this section, numerical results for the steady-state streamline and temperature contours within the partitioned enclosure for various values of the Rayleigh number Ra, inclination angle α and the dimensionless partition height B will be reported. In addition,

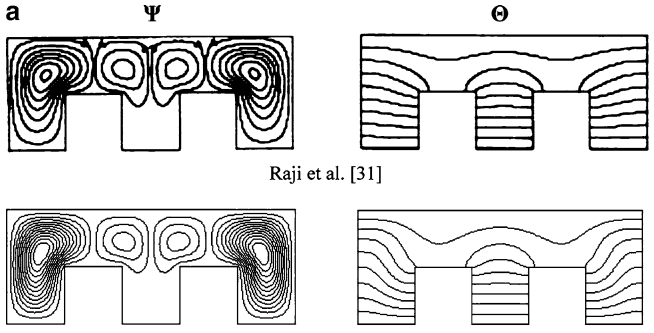

Comparison of present work with that of Raji et al. [31] for B=0.5, Pr=0.72, Ra=10^4 and α=0°.

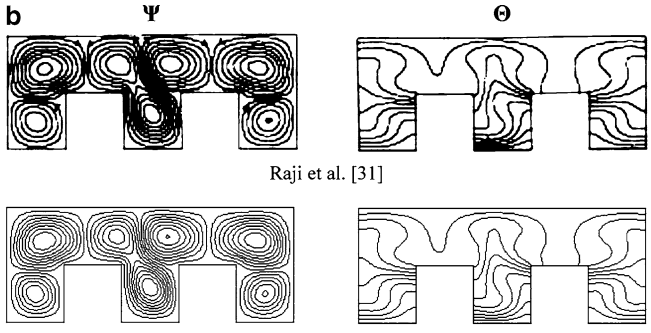

Comparison of present work with that of Raji et al. [31] for B=0.5, Pr=0.72, Ra= 5×10^4 and α=0°.

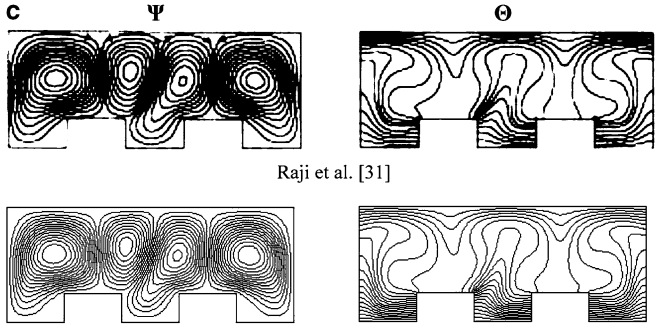

Comparison of present work with that of Raji et al. [31] for B=0.25, Pr=0.72, Ra= 5×10^4 and α=0°.

Fig. 2 **a** Comparison of present work with that of Raji et al. [31] for $B=0.5$, $\mathrm{Pr}=0.72$, $\mathrm{Ra}=10^4$ and $\alpha=0°$. **b** Comparison of present work with that of Raji et al. [31] for $B=0.5$, $\mathrm{Pr}=0.72$, $\mathrm{Ra}=5\times10^4$ and $\alpha=0°$. **c** Comparison of present work with that of Raji et al. [31] for $B=0.25$, $\mathrm{Pr}=0.72$, $\mathrm{Ra}=5\times10^4$ and $\alpha=0°$

representative results for the $\overline{Nu}$ for various conditions will be presented and discussed. These results correspond to free convective flow of air (Pr = 0.72) confined in a partitioned enclosure of aspect ratio of 2.5 subject to a transverse temperature gradient across the non-adiabatic walls of the enclosure.

Figure 3 presents steady-state contour plots for the streamline and temperature for various values of the Rayleigh number Ra with $B = 0.5$ and $\alpha = 0°$. For small Rayleigh numbers ($Ra = 10^3$), the free convection currents are small and the streamline contours exhibit a primary cell consisting of three weak secondary recirculating cells extending throughout the partitioned enclosure. The temperature contours within the enclosure are almost vertical and show little activity in the core of the enclosure indicating the existence of a quasi-conduction regime. As the Rayleigh number increases due to increased transverse temperature gradient, the convection currents increase causing the primary recirculation cell to rotate faster in the clockwise direction and to be stretched more and more towards the heated wall. This causes more flow to exist in the region close to the hot wall resulting in more flow in the small cavity made by the first partition close to the heated wall. This is evident from the increases in the value of the extreme stream function as Ra increases. This increased flow within the whole partitioned enclosure is accompanied by significant distortion in the temperature contours especially in the core of the enclosure as well as the non-adiabatic walls. For relatively high Rayleigh numbers ($Ra = 10^6$), the temperature contours are almost horizontal and show significant boundary-layer effects. This behavior has the tendency to increase the overall wall-heat transfer as will be shown later.

Figure 4 illustrates the effects of the enclosure inclination angle α on the contour maps of the streamlines and temperature for $B = 0.5$ and $Ra = 10^5$. For $\alpha = 0°$ (non-inclined partitioned enclosure), a primary stretched recirculating cell or vortex composing of three weaker secondary cells exists in the whole partitioned enclosure. As the enclosure is tilted, the recirculation speed within the enclosure tends to

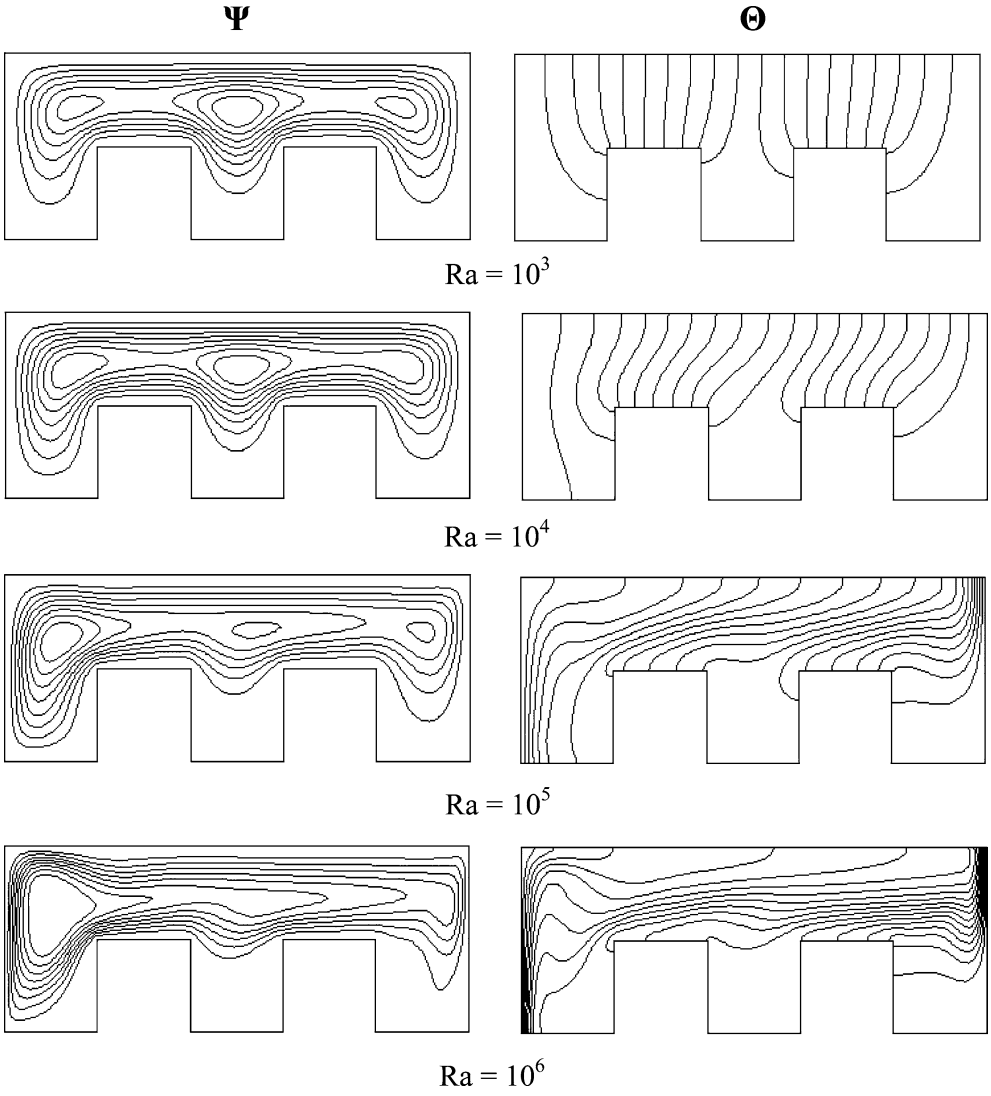

Fig. 3 Effects of Rayleigh number on the stream function and temperature contours. $B = 0.5$, Pr = 0.72 and $\alpha = 0°$

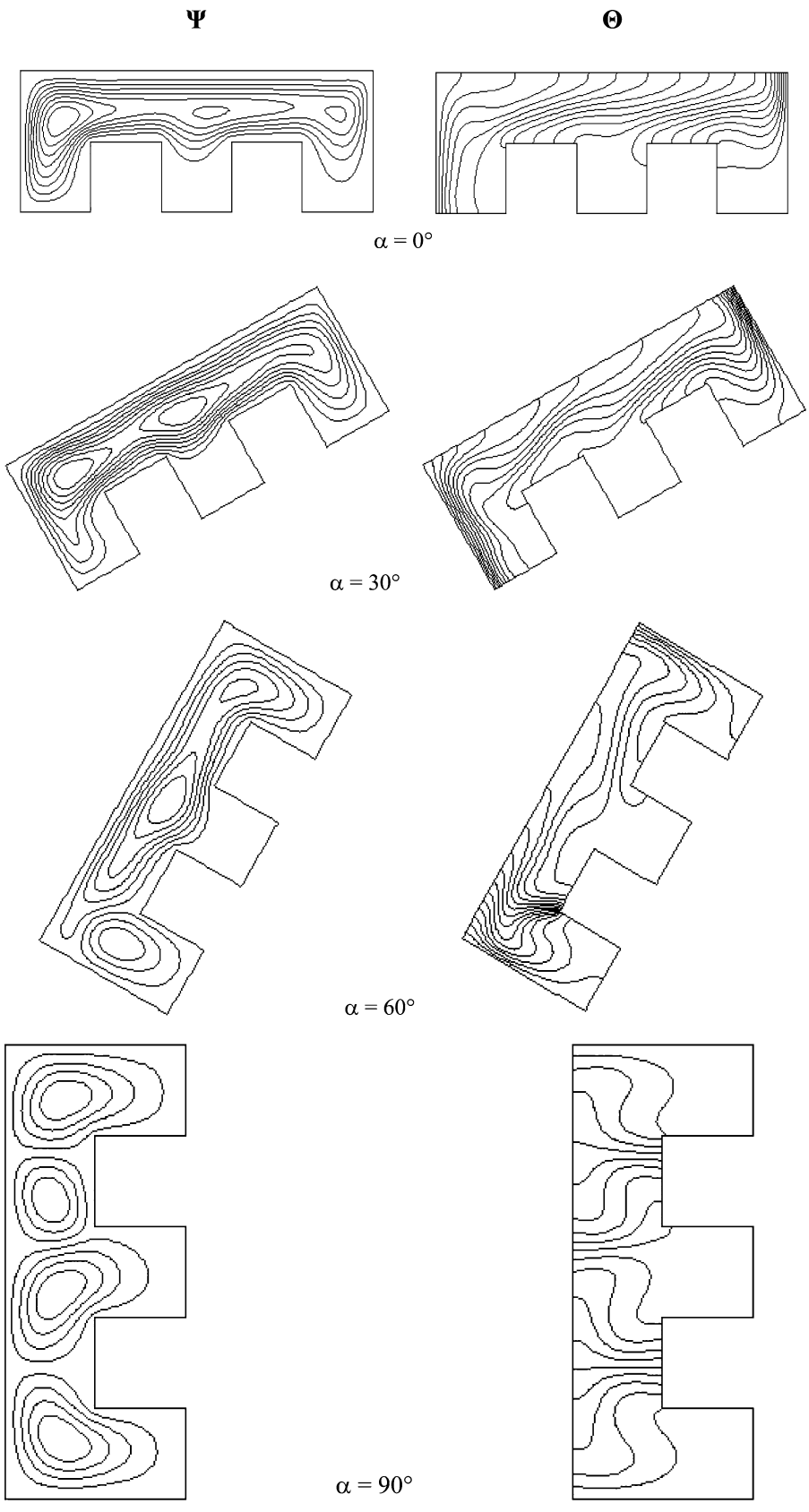

Fig. 4 Effects of inclination angle on the stream function and temperature contours. $B = 0.5$, $\mathrm{Pr} = 0.72$ and $\mathrm{Ra} = 10^5$

increase and the secondary vortices within the partitioned enclosure starts to separate. For example, when $\alpha = 60°$, a separated cell is predicted close to the heated wall while the other two vortices remain connected. Further tilting of the enclosure until $\alpha = 90°$, the two vortices break up and become distinctive. In addition,

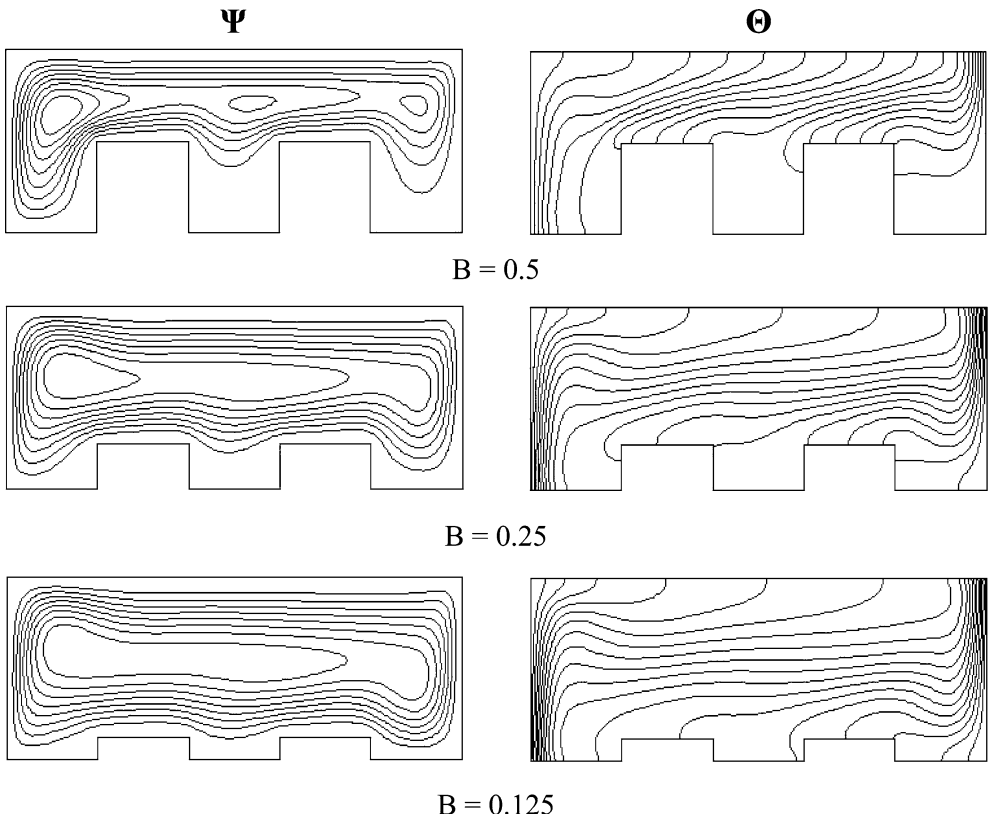

Fig. 5 Effects of B on the stream function and temperature contours. $Pr = 0.72$, $Ra = 10^5$ and $\alpha = 0°$

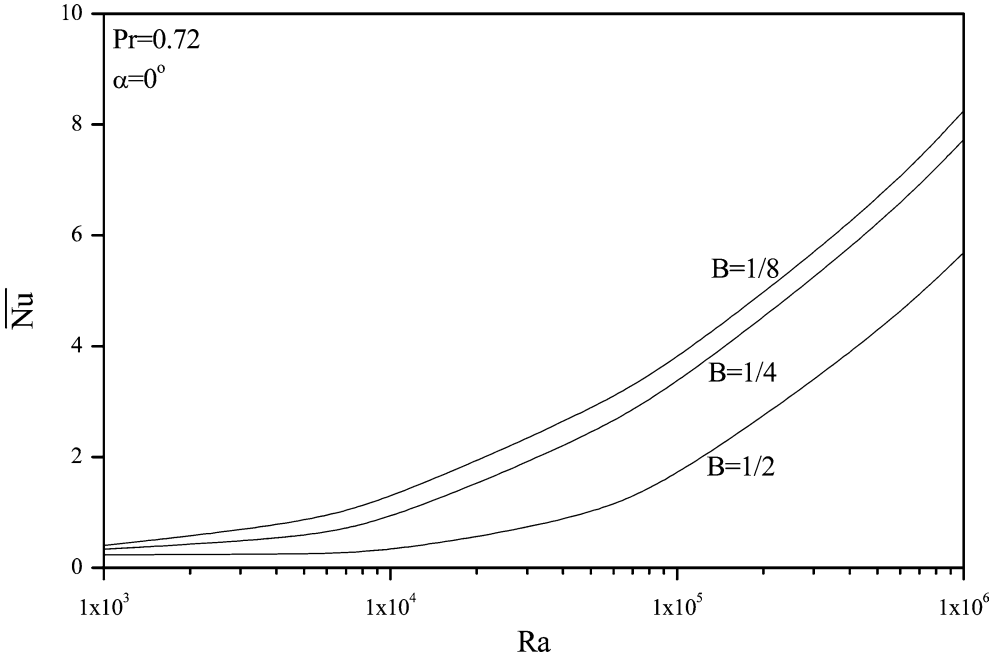

Fig. 6 Effect of B and Ra on the average Nusselt number

as the enclosure inclination angle changes from 60° to 90°, an additional small vortex forms within the core of the enclosure. Thus, for the case when $\alpha = 90°$, four separated recirculating cells are predicted. Furthermore, for $\alpha = 0°$ the isotherms are somewhat uniform and parallel to the insulated walls. For $\alpha = 30°$, they become more crowded close to the heated and cooled walls away from the core region of the partitioned enclosure with some distortion in the core region of the enclosure. However, for $\alpha = 60°$, the isotherms show a behavior of significant distortion in the boundary-layer region close to the heated wall while they remain

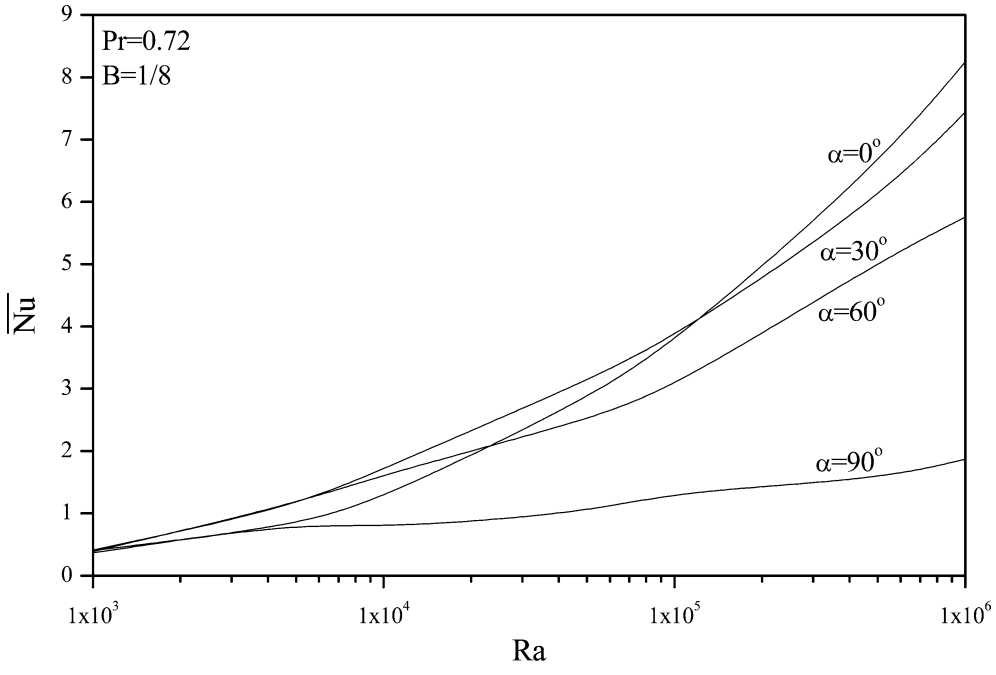

Fig. 7 Effects of α and Ra on the average Nusselt number for $B = 1/8$

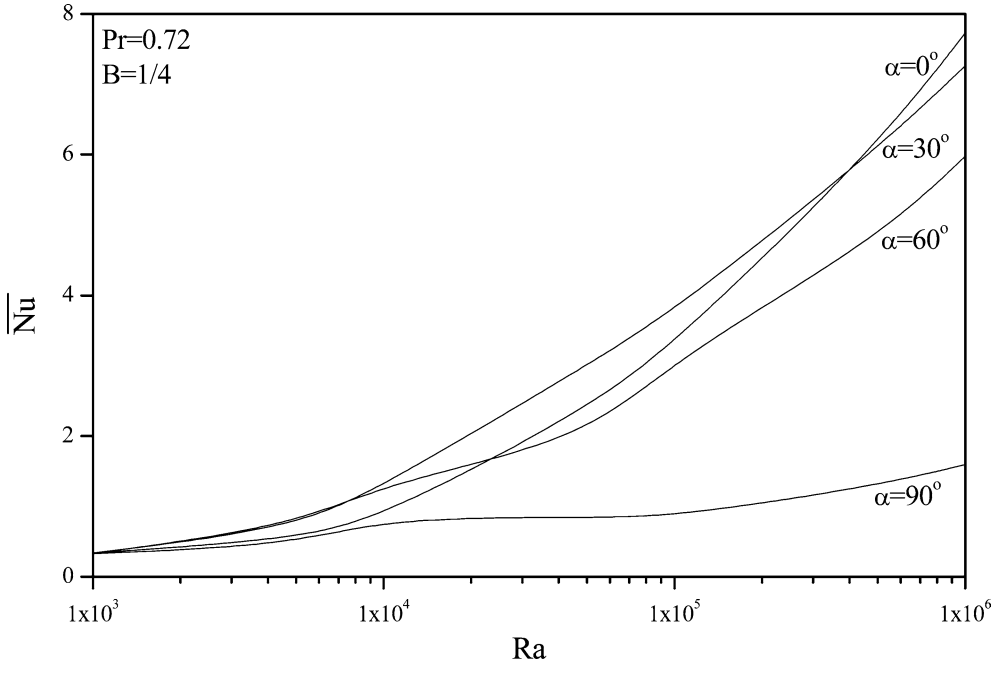

Fig. 8 Effect of α and Ra on the average Nusselt number for $B = 1/4$

somewhat more uniform in the partitioned enclosure core region. The distorting isotherms behavior close to the heated wall is associated with the existence of a separated vortex interacting with two connected vortices as discussed before. For $\alpha = 90°$, the degree of distortion in the isotherms behavior increases considerably within the whole partitioned enclosure. This is associated with the existence of four distinctive cells as mentioned before. In general, it is predicted that inclination of the partitioned enclosure has the effect of exhibiting a multi-cellular structure. The number of recirculating cells is a function of the enclosure inclination angle for the same parametric values of B, Pr and Ra.

Figure 5 depicts the influence of the dimensionless partition height B on the contour maps of the streamlines and temperature. When $B = 0.125$, a single clockwise recirculating cell or vortex stretched within the whole enclosure exists and the isotherms in the core region of the enclosure are parallel to the insulated walls indicating strong convection currents. As B increases to 0.25, the streamlines become squeezed within the

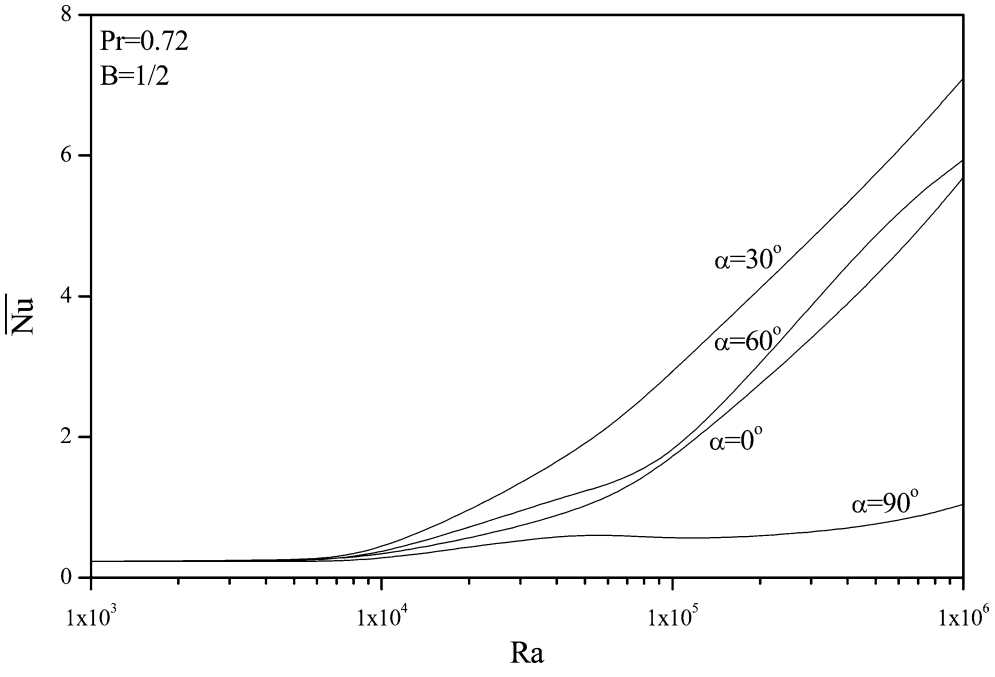

Fig. 9 Effect of α and Ra on the average Nusselt number for $B = 1/2$

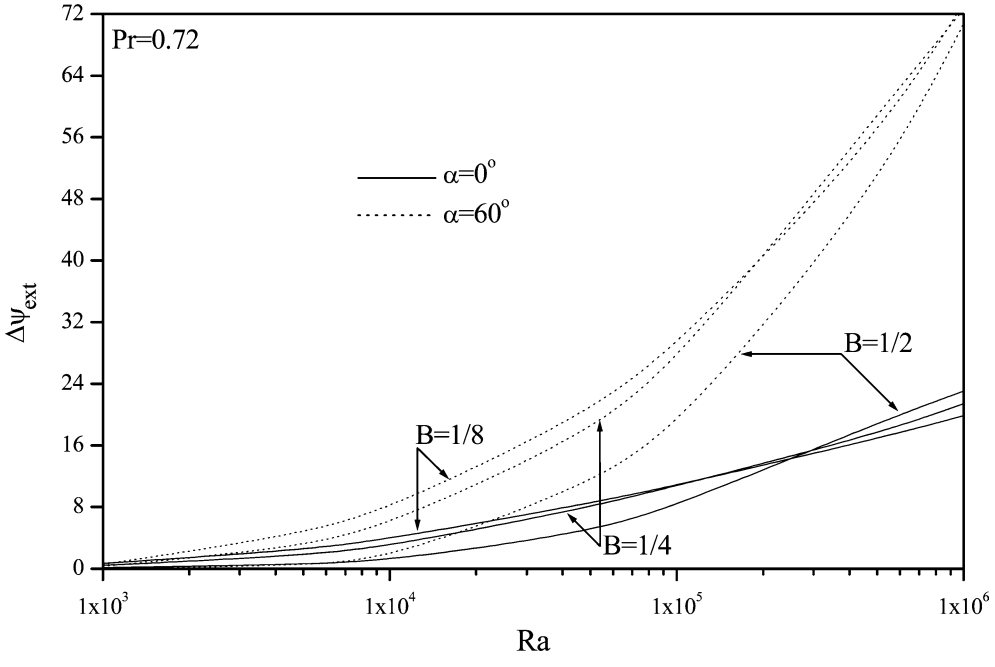

Fig. 10 Effects of B, Ra and α on the difference of extreme stream-function values

enclosure and tend to rotate at a lower speed. They also exhibit the formation of a secondary cell within the primary vortex close to the heated wall. For this case, the isotherms within the core region of the partitioned enclosure become less parallel to the insulated walls depicting less convective flow and therefore, less heat transfer at the heated wall. As B is increased further reaching 0.5, three secondary cells are formed within the primary vortex due to further squeezing of the flow and the isotherms in the core region are uniform but much less parallel to the insulated walls. The squeezing of the convective flow in the enclosure causes the air within the enclosure to rotate at lower speed and the heat transfer at the heated wall decreases as well. These behaviors are clearly illustrated in Fig. 5.

Figure 6 illustrates the effects of both Ra and B on the $\overline{\mathrm{Nu}}$ at the heated wall for a partitioned enclosure with no inclination. As mentioned before, increasing the Rayleigh number Ra produces higher buoyancy-induced flow within the enclosure and therefore, higher heat transfer at the heated wall. The degree of heat transfer enhancement is greater for greater values of Ra.

However, as the dimensionless partition height B increases, the flow speed within the partitioned enclosure decreases resulting in less wall heat transfer. These behaviors are depicted in the increases and decreases in the $\overline{Nu}$ as Ra and B increases, respectively, as evident from Fig. 6.

Finally, Figs. 7–9 present the effects of the partitioned enclosure inclination angle α on the $\overline{Nu}$ for the three different values of $B = 1/8$, $1/4$ and $1/2$, respectively. It is observed that the Rayleigh numbers for which the convection mode arises increases as B increases. Different behaviors in the profiles of $\overline{Nu}$ with Ra are observed depending on the value of B. For $B = 1/8$ and $B = 1/4$ the values of $\overline{Nu}$ decrease as α increases for values of $Ra > 2\times10^5$ for $B = 1/8$ and $Ra > 4\times10^5$ for $B = 1/4$. While this trend is the same for lower values of Ra for which the values of $\overline{Nu}$ decrease with increases in the values of $\alpha > 30°$, it is not the same for $\alpha = 0°$ in which $\overline{Nu}$ is lower than that corresponding to $\alpha = 30°$ (and for some cases $\alpha = 60°$) for the same value of Ra. These behaviors are associated with the fact that inclination of the partitioned enclosure in large amounts ($\alpha = 90°$) has the effect of forming a multi-cellular structure. In general, the separation of cells induces a further increase in the viscous forces between the vortices located close to the heated wall of the enclosure. Consequently, the corresponding $\overline{Nu}$ decrease. However, for relatively smaller Rayleigh numbers and angles between 30° and 60° and values of B between 1/8 and 1/4, the main vortex in the enclosure remains connected and rotates at a faster rate than that of the non-inclined case ($\alpha = 0°$). This results in higher average Nusselt numbers. These trends are clear from Figs. 7 and 8. For $B = 1/2$, the $\overline{Nu}$ decreases as α increases beyond 30° for all considered values of Ra. However, the values of $\overline{Nu}$ for $\alpha = 0°$ are lower than those of $\alpha = 30°$ and $\alpha = 60°$ for the whole range of Ra values considered in the study as shown in Fig. 9. It can be concluded from Figs. 7–9 that the $\overline{Nu}$ is strongly dependent on the inclination angle.

Figure 10 illustrates the effects of B and Ra on the difference of extreme stream-function values $\Delta\psi_{ext}$ for the two different conditions $\alpha = 0°$ (non-inclined partitioned enclosure) and $\alpha = 60°$ (inclined partitioned enclosure). As expected, as the Rayleigh number increases, the convection currents due to buoyancy-effects increases causing more induced flow. This results in higher values of $\Delta\psi_{ext}$. This is true regardless of the value of B as is obvious from Figure 10. Also, as mentioned before, inclination of the partitioned enclosure by 60° from the non-inclined position causes the flow recirculation speed within the enclosure to increase. This is reflected by the increase in $\Delta\psi_{ext}$ as α increases for all considered values of B in Fig. 10. Furthermore, in general, as B increases, $\Delta\psi_{ext}$ decreases since increasing the partition height presents obstacle to flow. However, for Ra values greater than 2×10^5 the values of $\Delta\psi_{ext}$ do not follow this trend depending of the value of α. For $\alpha = 0°$ and $Ra > 2\times10^5$, the values of $\Delta\psi_{ext}$ increase as B increases. On the other hand, when $\alpha = 60°$ and $Ra > 2\times10^5$, the values of $\Delta\psi_{ext}$ for $B = 1/8$ lie between those corresponding to $B = 1/4$ and $B = 1/2$. These behaviors are obvious from Fig. 10. It can be concluded from Fig. 10 that the wall heat transfer is also strongly dependent on the value of B.

5 Conclusions

Natural convective airflow in an inclined enclosure with partitions of different heights due to a transverse temperature gradient was studied numerically. The governing equations for this investigation were put in the dimensionless vorticity-stream function formulation and were solved by the finite volume method. Graphical results for the streamline and temperature contours as well as the Nusselt number for various parametric conditions were presented and discussed. A multi-cellular streamline structure was predicted for enclosure inclination angles between 60° and 90°. Also, it was predicted that the wall heat transfer and the flow characteristics inside the partitioned enclosure depended strongly on the dimensionless partition height, Rayleigh number and the enclosure inclination or tilting angle. It was found that the average Nusselt number increases with increase in the Rayleigh number. Also, as the dimensionless partition height increases, the flow speed within the partitioned enclosure decreases resulting in less wall heat transfer. In addition, the average Nusselt number was predicted to decrease as the partitioned enclosure inclination angle was increased beyond 30°. However, a different trend in the values of the average Nusselt number was predicted for an untilted enclosure depending on the value of the dimensionless partition height. It is hoped that the results obtained in the present work be useful for design and validation purposes.

References

1. Bejan A (1984) Convection heat transfer. Wiley, New York, NY
2. Platten JK, Legros JC (1984) Convection in liquids. Springer, Berlin Heidelberg New York
3. Yang KT (1987) Natural convection in enclosures. In: Kakac S, Shah R, Aung W (eds) Hand book of single phase convective heat transfer, New York
4. De Vahl Davis G, Jones IP (1983) Natural convection of air in a square cavity: a comparison exercise. Int J Numer Meth Fluids 3:227–248
5. Jones IP (1979) A comparison problem for numerical methods in fluid dynamics: the double glazing problem. In: 1st international conference for numerical methods in thermal problems, Swansea, UK, pp 338–348
6. Saitoh T, Hirose K (1989) High-accuracy benchmark solutions to natural convection in a square cavity. Comput Mech 4:417–427
7. De Vahl Davis G (1983) Natural convection of air in a square cavity: a Benchmark solution. Int J Numer Meth Fluids 3:249–264
8. Chenoweth DR, Paolucci S (1986) Natural convection in an enclosed vertical air layer with large horizontal temperature differences. J Fluid Mech 169:173–210

9. Paolucci S, Chenoweth DR (1989) Transition to chaos in a differentially heated vertical cavity. J Fluid Mech 201:379–410
10. Le Quere P, De Roquefort A (1985) Computation of natural convection in two-dimensional cavities with Chebyshev polynomials. J Comput Phys 57:210–228
11. Gresho PM, Lee RL, Chan ST, Sani RL (1979) Solution of the time-dependent incompressible Navier-Stokes and Boussinesq equations using the Galerkin finite element method. In: Proceedings of the IUTAM symposium on approximate methods for Navier-Stokes problems, Paderborn, West Germany, September, pp 203–222
12. Marshall RS, Heinrich JC, Zienkiewicz OC (1978) Natural convection in a square enclosure by a finite-element penalty function method using primitive fluid variables. Numer Heat Transf, 315–330
13. Usmani AS (1991) Finite element modeling of convective-diffusive heat transfer and phase transformation with reference to casting simulation. Ph.D. Thesis, University College of Swansea
14. Catton I (1972) Effect of wall conduction on the stability of a fluid in a rectangular region heated from below. J Heat Transf 94:446–452
15. Catton I (1979) Natural convection in enclosures. In: Proceedings of the 6^{th} international heat transfer conference, vol. 6, Toronto, pp 13–43
16. Oertel H (1978) Steady and time dependent convection in a rectangular box. In: Sixth international heat transfer conference, vol 2, pp 281–306
17. Torrance KE (1979) Natural convection in thermally stratified enclosures with localized heating from below. J Fluid Mech 95:477–495
18. Kamotani Y, Wang LW, Ostrach S (1983) Natural convection heat transfer in a water layer with localized heating from below. In: 21st national heat transfer conference, Seattle, HTD, vol. 26, pp 43–48
19. Fusegi T, Farouk B (1985) Natural convection in a thermally stratified square cavity with localized heating from below. In: 23rd AIChE national heat transfer conference, Denver, CO, Paper 85-HT-34
20. Markham BL, Rosenberger F (1984) Diffusive-Convective Vapor Transport Across Horizontal and Inclined Rectangular Enclosures. J Cryst Growth 67:241
21. Bontoux P, Smutek C, Randriamampianina A, Roux B, Extremet GP, Hurford AC, Rosenberger F, De Vahl Davis (1986) Numerical solutions and experimental results for three-dimensional buoyancy driven flows in tilted cylinders. Adv Space Res, Pergamon, New York, p 155
22. Delgado-Buscalioni R, Crespo del Arco E (2001) Flow and heat transfer regimes in inclined differentially heated cavities. Int J Heat Mass Transf 44:1947–1962
23. Lock GSH, Fu J (1993) Natural convection in the inclined cranked thermosyphon. J Heat Transfer 115:167–172
24. Wirtz RA, Tsheng WF (1980) Natural convection across tilted rectangular enclosures of small aspect ratio. In: Catton J, Torrance KE (eds) Natural convection in enclosures, vol. 8, ASME, New York, pp 54–67
25. Wirtz RA, Tsheng WF (1979) Finite difference simulation of free convection in tilted enclosures of low aspect ratio. In: Lewis, Morgan (eds) Numerical methods in thermal problems I, Pineridge, Swansea, UK, pp 381–390
26. Cerisier P, Rahal S (1995) Experimental study of the competition between convective rolls in an enclosure. In: Annie Steinchen (eds) Dynamics of Multiphase flows across interfaces. Pergamon, Oxford, pp 105
27. Jacobs HR, Mason WE, Hikida ET (1974) Natural convection in open rectangular cavities. Paper NC 3.2, Heat Transf 3:90–104
28. Jacobs HR, Mason WE (1976) Natural convection in open cavities with adiabatic sidewalls. Proceedings heat transfer and fluid mechanical institute, Stanford University Press, pp 33–46
29. Hasnaoui M, Bilgen E, Vasseur P (1990) Natural convection above an array of open cavities heated from below. Num Heat Transf, Part A 18:463–482
30. Jetli R, Acharya S, Zimmerman E (1986) Influence of Baffle location on natural convection in a partially divided enclosure. Numerical Heat Transfer 10:521–536
31. Raji A, Hasnaoui M, Zrikem Z (1997) Natural convection in Interacting Cavities Heated from Below. Int J Numer Meth Heat Fluid Flow 7:580–597
32. Dagtekin I, Oztop HF (2001) Natural convection heat transfer by heated partitions within enclosure. Int Commun Heat Mass Transf 28:823–834
33. Yucel N, Ozdem AH (2003) Natural convection in partially divided square enclosures. Heat Mass Transf 40:167–175
34. Patankar SV (1980) Numerical heat transfer and fluid flow. Hemisphere Publication Corporation, Washington